



HAL
open science

Structure and Dielectric Characteristics of Continuous Composition Spread Ba_{1-x}Sr_xTiO₃ Thin Films by Combinatorial Pulsed Laser Deposition

J. Qiu, G.Z. Liu, Jérôme Wolfman, C. Autret-Lambert, Sylvain Roger, J. Gao

► **To cite this version:**

J. Qiu, G.Z. Liu, Jérôme Wolfman, C. Autret-Lambert, Sylvain Roger, et al.. Structure and Dielectric Characteristics of Continuous Composition Spread Ba_{1-x}Sr_xTiO₃ Thin Films by Combinatorial Pulsed Laser Deposition. *Ceramics International*, 2016, 42 (5), pp.6408–6412. 10.1016/j.ceramint.2016.01.043 . hal-01757204

HAL Id: hal-01757204

<https://hal.science/hal-01757204>

Submitted on 8 Nov 2022

HAL is a multi-disciplinary open access archive for the deposit and dissemination of scientific research documents, whether they are published or not. The documents may come from teaching and research institutions in France or abroad, or from public or private research centers.

L'archive ouverte pluridisciplinaire **HAL**, est destinée au dépôt et à la diffusion de documents scientifiques de niveau recherche, publiés ou non, émanant des établissements d'enseignement et de recherche français ou étrangers, des laboratoires publics ou privés.

Structure and dielectric characteristics of continuous composition spread Ba_{1-x}Sr_xTiO₃ thin films by combinatorial pulsed laser deposition

J. Qiu¹, G. Z. Liu^{1*}, J. Wolfman², C. Autret-Lambert², Sylvain Roger², J. Gao¹

¹School of Mathematics and Physics, Suzhou University of Science and Technology,
Suzhou 215009, China

²Laboratoire GREMAN, UMR 7347 CNRS, Université François Rabelais, Parc de
Grandmont 37200 Tours, France

Email : guozhen.liu@hotmail.com

Abstract

Ba_{1-x}Sr_xTiO₃ ($0 \leq x \leq 1$, BST- x) continuous composition spread thin films were grown on SrTiO₃ substrates buffered by La_{0.9}Sr_{1.1}NiO₄ (LSNO) electrodes using combinatorial pulsed laser deposition. The effects of Sr concentration on the structure and dielectric properties of the Au/BST- x /LSNO capacitors were investigated. X-ray diffraction patterns and reciprocal space maps revealed that both the in-plane and out-of-plane BST- x lattice parameters decreased with the increment of Sr content. Impedance measurements showed that the dielectric constant and tunability simultaneously changed with Sr concentration and reached the maximum at about $x = 0.5$, which is comparable to that of BST- x individual thin films or bulks. Our results showed the large potential of combinatorial method in optimizing materials composition and even finding new materials.

Keywords: B. X-ray methods; C. Dielectric properties; D. BaTiO₃ and titanates

*Corresponding Author: Dr. G. Z. Liu

Associate Professor

School of Mathematics and Physics

Suzhou University of Science and Technology, Suzhou 215009

China

Email: Guozhen.liu@hotmail.com

Phone: +86-0512-68412901

1. Introduction

Dielectric materials exhibit high dielectric permittivity, low dielectric loss and for some of them dielectric tunability [1]. Intensive efforts have been made on dielectric materials for their potential applications in microwave and multifunctional devices [2-3]. $\text{Ba}_{1-x}\text{Sr}_x\text{TiO}_3$ (BST- x) is one of the most famous dielectrics since the dielectric properties of BST- x solid solution can be tailored by varying the mole fraction of Sr. Moreover, the lattice constants of BST- x can also be continuously tuned by the Sr content, which makes it an appropriate buffer layer and dielectric for fabricating other multifunction devices. So far, much attention has been paid to the fabrication of BST- x compounds with different Ba/Sr ratios. BST- x ceramics with different compositions had been prepared by solid state reaction [4-5]. For BST- x thin film growth, several methods have been developed, such as pulsed laser deposition (PLD) [6], polymer-assisted deposition [7], rf magnetron sputtering [8], metal-organic chemical-vapor deposition [9], combinatorial rf sputtering [10] and combinatorial PLD [11]. Theoretical methods were also applied to study composition-dependent BST- x solid solutions [12-13].

Combinatorial PLD provides a chance to prepare continuous composition spread library on a single substrate at the same time [14-15], which means that the properties of the various compounds can be directly compared and solely depend on their local chemical composition, contrary to batch of successive experiments where influences from run-to-run fabrication parameters modulation cannot be ruled out. Although there are a few reports on BST- x films grown by combinatorial PLD, most of the BST- x films were grown directly on insulating LaAlO_3 or SrTiO_3 substrates, which are inconvenient for the investigation of their dielectric behaviors in metal-insulator-metal structure [11, 16]. In the current work, we successfully fabricated continuous composition spread Au/BST- $x/\text{La}_{0.9}\text{Sr}_{1.1}\text{NiO}_4$ capacitors by combinatorial PLD, and studied the structural and

dielectric properties of the BST- x based capacitors.

2. Experimental details

$\text{La}_{0.9}\text{Sr}_{1.1}\text{NiO}_4$ (LSNO) bottom electrode with thickness of 120 nm was first grown on (001) SrTiO_3 (STO, nominal size: 10 mm \times 10 mm) substrate by PLD technique, and then BST- x composition spread thin film library was deposited on LSNO layer by combinatorial PLD. The excimer laser wave length, fluence, and repetition rate are 248 nm, 2.0 J/cm², and 5 Hz, respectively. Both LSNO and BST- x thin films were deposited at 600 °C in an oxygen ambient pressure of 10 Pa. The BST- x thin films with a thickness of about 250 nm were grown by sequentially ablating stoichiometric STO and BaTiO_3 (BTO) ceramic targets. The deposition rate is about 33 pulses per unit cell for STO layer and 30 pulses per unit cell for BTO layer. More deposition description in detail was presented elsewhere [17]. Local compositions of BST- x thin films were identified by energy dispersive x-ray spectroscopy (EDX). In addition, local crystal structure were characterized by a high resolution x-ray diffractometer (HRXRD) equipped with a motorized x - y stage and the BST- x thin films were measured with a step of one millimeter along x direction. A 50- μm -width slit was used on the primary optic side of x-ray diffractometer to confine a 92- μm -width beam footprint on BST- x thin film surface along the x direction. The crystal structure and orientation were determined by XRD θ - 2θ scans. Two-dimensional x-ray reciprocal space mapping (RSM) around the STO (103) reflection was also performed to evaluate both the in-plane and out-of plane lattice parameters of the BST- x film. Through a shadow mask, Au top electrodes were deposited by dc magnetron sputtering for electrical measurements. The size of Au electrodes measured by

optical microscopy was about 180 μm and 500 μm in x and y direction, respectively. The dielectric properties were measured by a HP4294A impedance analyzer with an oscillator voltage of 30 mV at room temperature.

3. Results and discussion

3.1 compositional analysis

The compositions of the BST- x films were characterized by EDX and the results are shown in Fig.1. With respect to the concentration of Ti, the calculated Sr concentration varied almost linearly from zero at one side to 100 percent at the other side along x direction and kept nearly unchanged along y direction, which is consistent with the nominal values. The good agreement between the measured composition and desired composition indicates that the BST- x composition spread thin film library was successfully built on LSNO layer by combinatorial PLD method.

3.2 Structural analysis

Room temperature XRD θ - 2θ patterns of BST- x thin film around the (002) reflection of the STO substrate are shown in Fig.2. Except the (00 l) peaks of the STO substrate and the LSNO, BST- x films, there is also a small peak around 45 degree marked by asterisk, which probably arose from XRD sample stage. For each measurement, the nominal increment in Sr concentration across BST- x composition library is 0.11. With the increment in Sr content, the (002) diffraction peaks of the BST- x films shifted from 46.48° for STO to 44.72° for BTO, as indicated by the horizontal arrow. The obvious evolution of the (002) diffraction peaks for the BST- x films with the Sr concentration suggests

composition gradient BST- x films were successfully fabricated.

RSMs around asymmetrical (103) reflection of STO substrate were obtained every millimetre along x -axis of BST- x composition library. RSM on (103) can offer independent determination both in-plane and out-of-plane lattice parameters by taking the ratio of reciprocal lattice units of STO and BST- x spots in reciprocal space [18]. Figure 3 shows the RSMs of BST- x /LSNO/STO stack with $x = 0, 0.33, 0.67$ and 1. The h and l axes are parallel to the out-of-plane and in-plane directions of the film, respectively. The intensive spot ($h=1$ and $l=3$) arises from the STO substrate and the weak and dispersive spot with smaller h and l values is assigned to the (103) BST- x composition library. There is no spot from (103) LSNO observed in Fig. 3 due to the K_2NiF_4 type LSNO has a much longer c axis than that of STO and BST- x . In Fig. 3(a), the BST- x ($x=1$, STO) spot was lined up with STO (103) substrate spot along h axis, indicating the fabricated STO film has the same in-plane lattice parameter with the STO substrate. Compared with STO substrate, however, the STO film exhibited smaller l value and hence larger out-of-plane lattice constant, which is probably due to the slight deviation of the optimal growth conditions for stoichiometric STO film by PLD [19]. It can be seen that, with the decrease of Sr content, the values of h and l decreased, corresponding to the increment of both in-plane and out of plane lattice parameters of BST- x films.

The relationship between Sr concentration and lattice parameters of BST- x composition library is shown in Fig. 4. The out-of-plane and in-plane lattice parameters c and a were extracted from (103) RSMs and the c lattice parameter was also calculated

from BST- x θ - 2θ XRD patterns for comparison. With increasing Sr content x , in-plane lattice parameter decreased from 4.022 Å for $x = 0$ to 3.905 Å for $x = 1$. Similarly, out-of-plane lattice parameter descended from 4.051 Å for $x = 0$ to 3.910 Å for $x = 1$. Furthermore, the value of in-plane lattice parameter is always less than that of out-of-plane lattice parameter at a specific Sr content, meaning that the crystal structure of BST- x composition thin film library is tetragonal, which is in accordance with previous reports [7].

3.3 Dielectric properties

It should be noted that the presence of interfacial capacitance between LSNO and BST- x films may affect the capacitance measurement at high frequencies [20]. Therefore, a contour plot of capacitance over a xy position plane was given at a low frequency of 5 kHz as shown in Fig. 5. Obviously, the capacitance values were almost constant along y direction and gradually changed along x direction. The capacitance map is similar to the desired composition map which is constant along y direction and spread along x direction, suggesting that composition spread BST- x films were fabricated successfully on LSNO/STO by combinatorial PLD method due to the sensitivity of the capacitance (permittivity) of BST- x to the Ba/Sr ratio [6]. According to the map, the capacitance rose steadily from about 2.25 nF at BTO side up to around 5.96 nF in the center region, and then decreased to 0.97 nF at STO side. The distribution of capacitance in BST- x library revealed the change of the local composition in BST- x layer, considering the negligible change of interfacial capacitance across the BST- x composition library.

Based on the contour plot of capacitance, the mean capacitance as a function of Sr concentration is summarized. In addition, the relative permittivity ϵ_r of BST- x composition library was derived from the mean capacitance C according to the following equation: $C=A\epsilon_r\epsilon_0/d$, where A represents the area of capacitors, ϵ_0 is the dielectric permittivity of vacuum, and d is the thickness of films. Figure 6 shows the dependence of the permittivity and the dielectric loss on Sr concentration. The permittivity and dielectric loss share the same variable trend. According to our previous measurement, the Curie temperature (T_c) of BST- x thin films at $x \approx 0.6$ is around room temperature [17]. So both the permittivity and the dielectric loss of BST- x thin films reached their maximum for the compounds having T_c around room temperature.

Figure 7(a) compares the capacitance-voltage (C - V) property of BST- x films with different Sr content at 5 kHz. Almost all the BST- x films measured showed butterfly C - V loops, especially for those with x ranging from 0.1~0.7, confirming the existence of ferroelectricity in part of the BST- x films. The dependence of tunability on Sr content of BST- x composition library is shown in Fig.7 (b). The relative tunability T_r is calculated based on the expression: $T_r = [C(0) - C(V)] / C(0) \times 100 \%$, where the $C(0)$ and $C(V)$ represent the capacitances of BST- x solid solution under zero and given bias, respectively. Similar to the dependences of dielectric permittivity and loss on Sr content, the tunability showed also a maximum of ~85% in the range of 0.4 to 0.5. Again obtaining higher tunability close to the Curie temperature was expected. Here, the observed relationships between dielectric permittivity, loss and tunability of BST- x films and Sr content are

similar to those for BST- x films grown by laser ablation and polymer-assisted deposition [6, 7], suggesting the films grown by combinatorial PLD can achieve the same quality as those grown by other methods.

4. Conclusions

In summary, BST- x composition spread thin film library was grown by combinatorial PLD and the structure and dielectric properties were investigated. The variation of local compositions across BST- x thin film library was consistent with nominal values. The local structural measurements revealed the dependence of both in-plane and out-of plane lattice parameters on Sr concentration of BST- x thin film library. The BST- x dielectric permittivity, loss and tunability increased first with Sr concentration x , and reached maximum at around 0.5, then decreased to a lower value, which is similar to the observations in individual BST- x bulks and thin films. Our results prove the effectiveness and convenience of combinatorial PLD in finding the best material performances compromise versus composition for a given application.

Acknowledgement

This work is supported by National Key Basic Research Program of China (Grant No. 2014CB921002), the National Natural Science Foundation of China (Grant Nos. 11304089 and 11374225) and the Scientific Research Foundation for the Returned Overseas Chinese Scholars, State Education Ministry. This work is also supported by the Priority Academic Program Development of Jiangsu Higher Education Institutions and the USTS Cooperative Innovation Center for Functional Oxide Films and Optical

Information.

References

- [1] A. K. Tagantsev, V. O. Sherman, K. F. Astafiev, J. Venkatesh, N. Setter, Ferroelectric materials for microwave tunable applications, *J. Electroceram.* 11 (2003) 5-66.
- [2] P. Bao, T. J. Jackson, X. Wang, M. J. Lancaster, Barium strontium titanate thin film varactors for room-temperature microwave device applications, *J. Phys. D: Appl. Phys.* 41 (2008) 063001.
- [3] K. J. Jin, H. B. Lu, K. Zhao, C. Ge, M. He, G. Z. Yang, Novel multifunctional properties induced by interface effects in perovskite oxide heterostructures, *Adv. Mater.* 21 (2009) 4636-4640.
- [4] J. N. Lin, T. B. Wu, Effects of isovalent substitutions on lattice softening and transition character of BaTiO₃ solid solutions, *J. Appl. Phys.* 68 (1990) 985-993.
- [5] L. Q. Zhou, P. M. Vilarinho, J. L. Baptista, Dependence of the structural and dielectric properties of Ba_{1-x}Sr_xTiO₃ ceramic solid solutions on raw material processing, *J. Euro. Ceram. Soc.* 19 (1999) 2015-2020.
- [6] Y. Gim, T. Hudson, Y. Fan, C. Kwon, A. T. Findikoglu, B. J. Gibbons, B. H. Park, Q. X. Jia, Microstructure and dielectric properties of Ba_{1-x}Sr_xTiO₃ films grown on LaAlO₃ substrates, *Appl. Phys. Lett.* 77 (2000) 1200-1202.
- [7] Y. Lin, Jang-Sik Lee, H. Wang, Y. Li, S. R. Foltyn, Q. X. Jia, G. E. Collis, A. K. Burrell, T. M. McClesdey, Structural and dielectric properties of epitaxial Ba_{1-x}Sr_xTiO₃ films grown on LaAlO₃ substrates by polymer-assisted deposition, *Appl. Phys. Lett.* 85 (2004) 5007-5009.

- [8] T. S. Kim, C. H. Kim, M. H. Oh, Structural and electrical properties of rf magnetron-sputtered $\text{Ba}_{1-x}\text{Sr}_x\text{TiO}_3$ thin films on indium-tin-oxide-coated glass substrate, *J. Appl. Phys.* 75 (1994) 7998-8003.
- [9] S. Regnery, Y. Ding, P. Ehrhart, C. L. Jia, K. Szot, R. Thomas, R. Waser, Metal-organic chemical-vapor deposition of (Ba, Sr) TiO_3 : Nucleation and growth on Pt-(111), *J. Appl. Phys.* 98 (2005) 084904.
- [10] H. Chang, C. Gao, I. Takeuchi, Y. Yoo, J. Wang, P. G. Schultz, X. D. Xiang, R. P. Sharma, M. Downes, T. Venkatesan, Combinatorial synthesis and high throughput evaluation of ferroelectric/dielectric thin-film libraries for microwave applications, *Appl. Phys. Lett.* 72 (1998) 2185-2187.
- [11] K. Terai, M. Lippmaa, P. Ahmet, T. Chikyow, T. Fuji, H. Koinuma, M. Kawasaki, In-plane lattice constant tuning of an oxide substrate with $\text{Ba}_{1-x}\text{Sr}_x\text{TiO}_3$ and BaTiO_3 buffer layers, *Appl. Phys. Lett.* 80 (2002) 4437-4439.
- [12] O. G. Vendik, S. P. Zubko, S. F. Karmanenko, M. A. Nikol'ski, N. N. Isakov, I. T. Serenkov, V. I. Sakharov, Layered planar capacitor based on $\text{Ba}_x\text{Sr}_{1-x}\text{TiO}_3$ with variable parameter x , *J. Appl. Phys.* 91 (2002) 331-335.
- [13] H. Wu, W. Z. Shen, Dielectric and pyroelectric properties of $\text{Ba}_x\text{Sr}_{1-x}\text{TiO}_3$: quantum effect and phase transition, *Phys. Rev. B* 73 (2006) 094115.
- [14] X. D. Xiang, X. Sun, G. Briceño, Y. lou, K. A. Wang, H. Chang, W. G. Wallace-Freedman, S. W. Chen, P. G. Schultz, A combinatorial approach to materials discovery, *Science* 268 (1995) 1738.

- [15] X. Y. Sun, C. Zhang, N. M. Aimon, T. Goto, M. Onbasli, D. H. Kim, H. K. Choi, C. A. Ross, Combinatorial pulsed laser deposition of magnetic and magneto-optical Sr (Ga_xTi_yFe_{0.34-0.40})O_{3-δ} perovskite films, ACS Comb. Sci. 16 (2014) 640-646.
- [16] J. W. Li, F. Duewer, C. Gao, H. Chang, X. D. Xiang, Electro-optic measurements of the ferroelectric-paraelectric boundary in Ba_{1-x}Sr_xTiO₃ materials chips, Appl. Phys. Lett. 76 (2000) 769-771.
- [17] G. Z. Liu, J. Wolfman, C. A. Lambert, J. Sakai, S. Roger, M. Gervais, F. Gervais, Microstructural and dielectric properties of Ba_{0.6}Sr_{0.4}Ti_{1-x}Zr_xO₃ based combinatorial thin film capacitors library, J. Appl. Phys. 108 (2010) 114108.
- [18] W. Wei, A. Sehirlioglu, Strain relaxation analysis of LaAlO₃/SrTiO₃ heterostructure using reciprocal lattice mapping, Appl. Phys. Lett. 100 (2012) 071901.
- [19] G. Z. Liu, Q. Y. Lei, X. X. Xi, Stoichiometry of SrTiO₃ films grown by pulsed laser deposition, Appl. Phys. Lett. 100 (2012) 202902.
- [20] G. Z. Liu, C. Wang, C. C. Wang, J. Qiu, M. He, J. Xing, K. J. Jin, H. B. Lu, G. Z. Yang, Effects of interfacial polarization on the dielectric properties of BiFeO₃ thin film capacitors. Appl. Phys. Lett. 92 (2008) 122903-122903.

FIGURE CAPTIONS

Figure 1. Local Sr concentration versus positions along x direction of samples with respect to the Ti and oxygen concentration.

Figure 2. Evolving θ - 2θ XRD patterns of BST- x /LSNO/STO stacks around (002) reflection of STO substrate with Sr concentration in BST- x layer.

Figure 3. RSMs around (103) reflection of STO substrate for BST- x /LSNO/STO stacks. The Sr concentrations x in BST- x layer are (a) $x= 1$, (b) $x= 0.67$, (c) $x=0.33$ and (d) $x= 0$, respectively.

Figure 4. Lattice-parameter dependence of BST- x on Sr concentration.

Figure 5. Contour plot of the capacitance of BST- x composition spread thin film library at 5 kHz.

Figure 6. Permittivity and dielectric loss of BST- x layer as a function of Sr concentration at 5 kHz.

Figure 7. (a) Capacitance–voltage characteristics at room temperature at 5 kHz for BST- x films, (b) the tunability dependence of BST- x layer on Sr concentration.

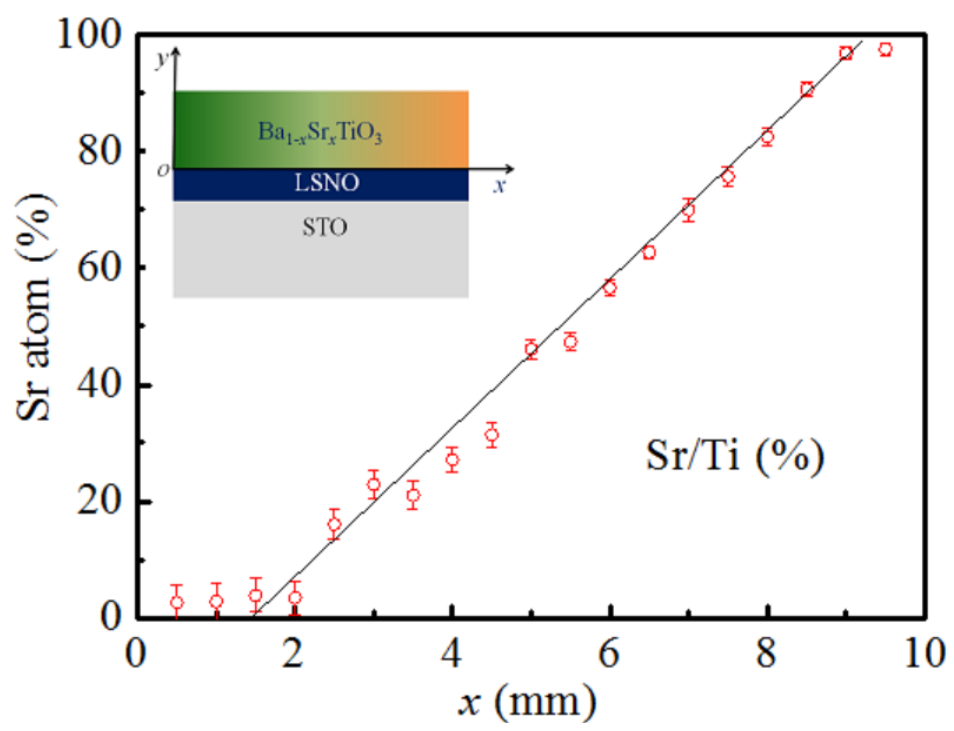


Figure 1

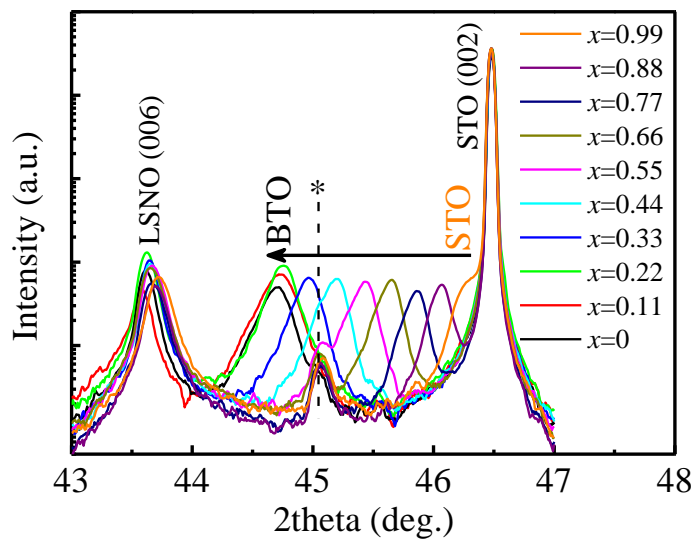


Figure 2

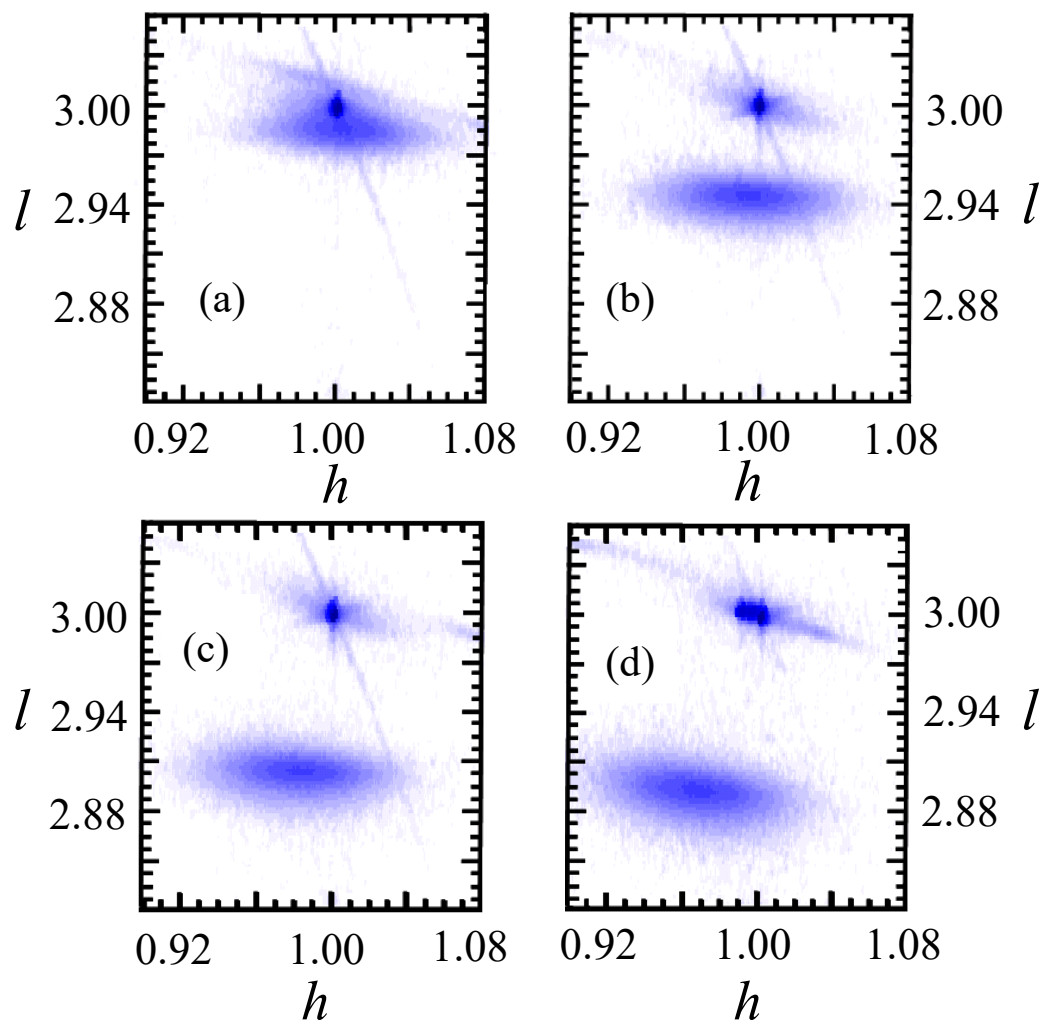


Figure 3

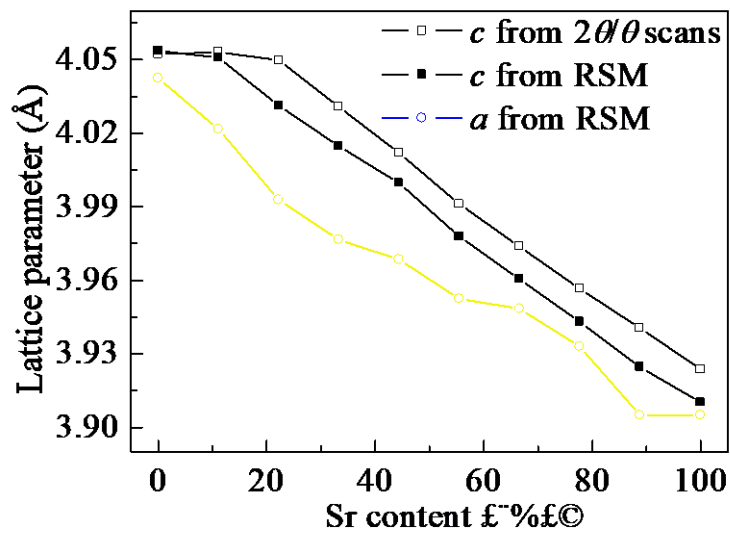


Figure 4

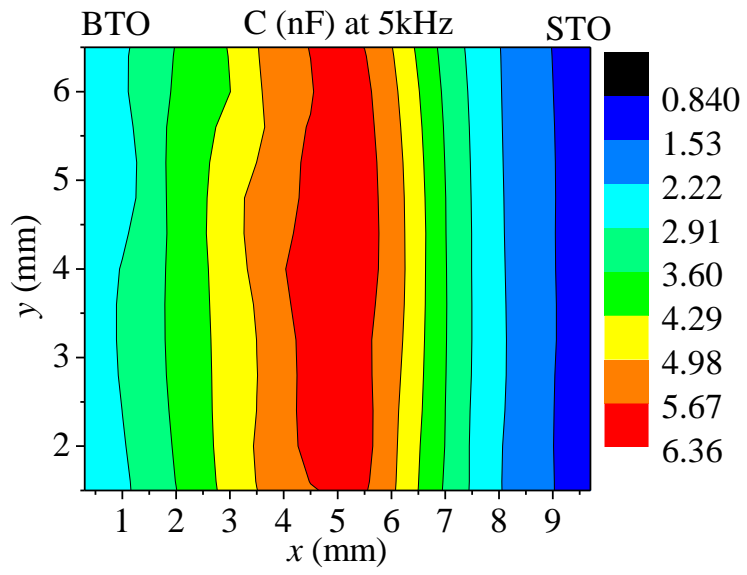


Figure 5

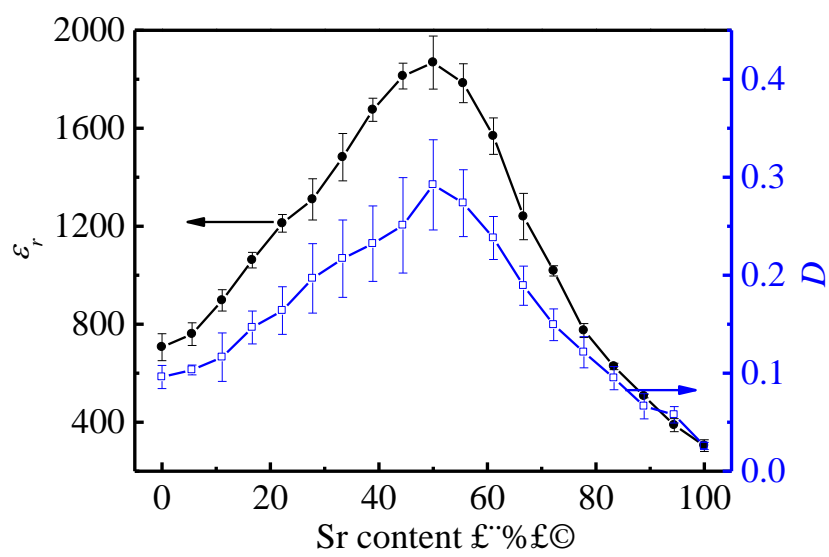


Figure 6

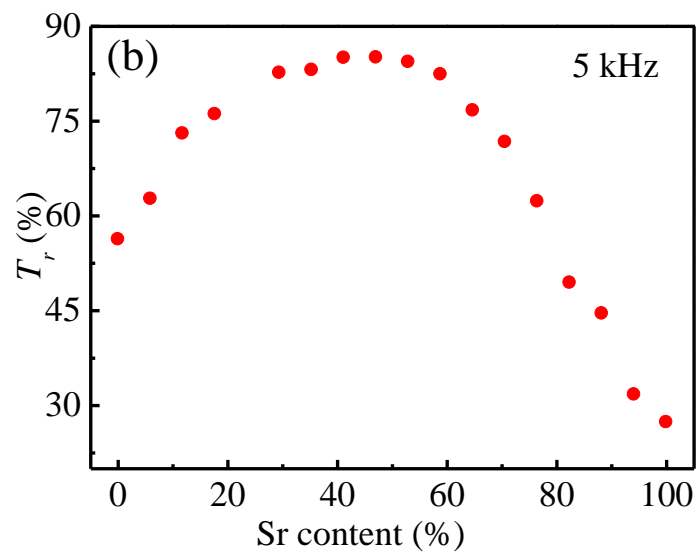
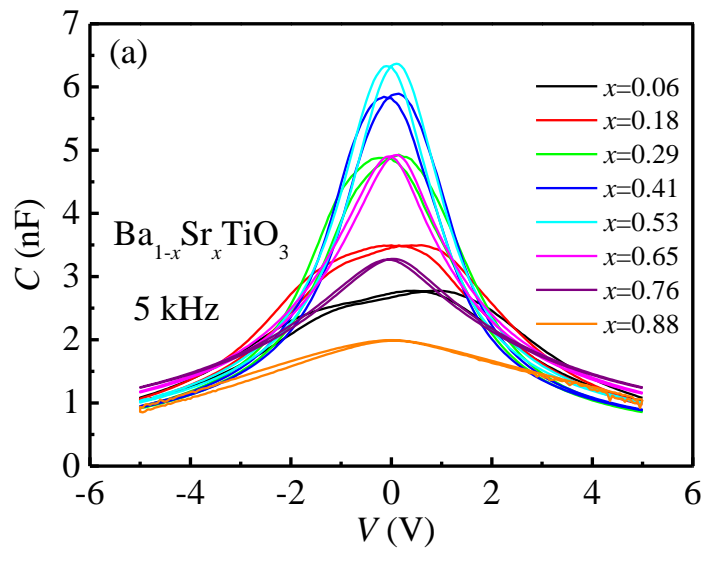


Figure 7